Impaired Development of Collagen Antibody-Induced Arthritis in Rab44-Deficient Mice

Yu Yamaguchi , Tomoko Kadowaki , Eiko Sakai , Mayuko Noguromi , Shun Oyakawa , Takayuki Tsukuba *

Posted Date: 18 September 2024

doi: 10.20944/preprints202409.1444.v1

Keywords: Rab44; collagen antibody-induced arthritis; immune cells; osteoclasts

Article

Impaired Development of Collagen Antibody-Induced Arthritis in Rab44-Deficient Mice

Yu Yamaguchi [1], Tomoko Kadowaki [2], Eiko Sakai [1], Mayuko Noguromi [1,2,3], Shun Oyakawa [1,3] and Takayuki Tsukuba [1,*]

[1] Department of Dental Pharmacology, Graduate School of Biomedical Sciences, Nagasaki University, Nagasaki 852-8588, Japan
[2] Department of Frontier Oral Science, Graduate School of Biomedical Sciences, Nagasaki University, Nagasaki 852-8588, Japan
[3] Department of Prosthetic Dentistry, Graduate School of Biomedical Sciences, Nagasaki University, Nagasaki 852-8588, Japan
* Takayuki Tsukuba: tsuta@nagasaki-u.ac.jp

Abstract: Rheumatoid arthritis (RA) is an autoimmune disease characterized by immune cell-mediated joint inflammation and subsequent osteoclast-dependent bone destruction. Collagen antibody-induced arthritis (CAIA) is a useful mouse model for examining the inflammatory mechanisms in human RA. Previously, we identified the novel gene Rab44, which is a member of the large Rab GTPase family and is highly expressed in immune-related cells and osteoclasts. In this study, we induced CAIA in Rab44-knockout (KO) mice to investigate the effects of Rab44 on inflammation, cell filtration, and bone destruction. Compared with wild-type (WT) mice, Rab44 KO mice showed reduced inflammation in arthritis under CAIA-inducing conditions. Rab44 KO CAIA mice exhibited reduced cell filtration in the radiocarpal joints. Consistent with these findings, Rab44-KO CAIA mice showed decreased mRNA levels of arthritis-related marker genes including inflammation, cartilage turnover, bone formation, and bone absorption markers. Rab44-KO CAIA mice exhibited predominant infiltration of M2-type macrophages at inflammatory sites and reduced bone loss compared to WT CAIA mice. These results indicate that Rab44 deficiency reduces the progression of inflammation in CAIA in mice.

Keywords: Rab44; collagen antibody-induced arthritis; immune cells; osteoclasts

1. Introduction

Rheumatoid arthritis (RA) is a chronic autoimmune disease characterized by inflammation of the synovial membrane, leading to joint swelling, pain, and eventual destruction of the cartilage and bone [1]. In the pathogenesis of RA, the misrecognition of self-antigens produces B cell-mediated autoantibodies and induces T cell-mediated stimulation of macrophages and synovial fibroblasts for conversion into tissue-destructive cells [2,3]. Subsequently, the activated cells produce various inflammatory mediators to facilitate osteoclast-dependent bone destruction [4,5]. Because these processes are highly complex, several animal models are available to mimic the pathological conditions of human RA. Collagen antibody-induced arthritis (CAIA) is well investigated using a mouse model, which is induced by intravenous injection of collagen II antibodies followed by injection with the adjuvant booster lipopolysaccharides (LPS) [6,7]. CAIA is useful not only for examining inflammatory mechanisms in RA but also for screening new therapeutics for regulating inflammatory events in RA [8]. Therefore, performing CAIA experiments in knockout (KO) mice is a powerful tool for analyzing individual gene functions in RA.

Rab GTPases are major regulators of intracellular membrane trafficking [9–11]. Rab44 is a member of "large" Rab GTPases and different from conventional "small" Rab GTPases, which include Rab1-43 with low molecular weights of approximately 20–30 kDa [12,13]. Rab44 possesses additional domains, the EF-hand, coiled-coil, and proline-rich domains at the N-terminus, and a Rab

 doi:10.20944/preprints202409.1444.v

domain at the C-terminus with molecular weights of approximately 70–150 kDa [14,15]. Rab44 upregulates during osteoclast differentiation [14] and is highly expressed in immune-related cells, such as mast cells and granulocyte-lineage cells in the bone marrow [16,17]. Previous studies have reported that Rab44-knockout (Rab44-KO) mice displayed reduced anaphylactic responses and impaired nickel-induced hypersensitivity *in vivo* [18–20]. Moreover, in *in vitro* experiments, mast cells from Rab44-KO mice exhibited decreased secretion of histamine and lysosomal enzymes compared to cells from wild-type mice [17,18]. In macrophages, Rab44 knockdown enhances osteoclast differentiation, whereas Rab44 overexpression prevents osteoclast differentiation [14]. Considering that Rab44 has been implicated in the function and differentiation of immune cells and osteoclasts, Rab44 may play an important role in RA development. However, the involvement of Rab44 in the development of RA remains unknown.

In this study, we induced CAIA in Rab44-KO mice to investigate the effects of Rab44 on inflammation, cell filtration, and bone destruction in CAIA.

2. Materials and Methods

2.1. Antibodies and reagents

The rabbit polyclonal anti-CD68 antibody (Cat. no. ab125212) was purchased from Abcam (Cambridge, UK). The CD80 polyclonal antibody (Cat. no. bs-2211R) was purchased from Bioss (MA, USA). The CD206 rabbit monoclonal antibody (Cat. no. 24595) was obtained from Cell Signaling Technology (MA, USA). ArthritoMAB™ antibody cocktail for C57BL/6 (Cat. no. CIA-MAB-2C) and lipopolysaccharide (LPS) (Cat. no. MDLPS5-0) were obtained from MDB (Zürich, Switzerland).

2.2. Animals

Rab44-KO mice were generated from C57BL/6 background mice using a CRISPR/Cas9-mediated genome editing method described previously [21]. All animal experiments were conducted using age-matched (8-12 weeks old) female wild type (WT) and Rab44-KO littermate mice. The number of mice used is indicated as "n" in the respective figure legends. All animal experimental protocols were approved by the Animal Experiment Committee of the Graduate School of Biomedical Sciences, Nagasaki University (permit number: 2107211733).

2.3. Induction of Collagen Antibody-Induced Arthritis (CAIA)

The age-matched (8-12 weeks old) female mice were intraperitoneally injected with 2 mg ArthritoMab arthritis-inducing antibody cocktail on day 0. Three days after of the initial administration, the mice were intraperitoneally boosted with 50 μg LPS. The control group was intraperitoneally injected with phosphate-buffered saline (PBS) on days 0 and 3. All mice were monitored for 9 days, and arthritis development was scored. A maximum of 16 points were assigned, with 4 points per paw (no swelling, 0 points; mild swelling and/or one swollen joint, 1 point; moderate swelling and/or two swollen joints, 2 points; marked swelling and/or all swollen joints, 3 points; and severe swelling with redness and all swollen joints, 4 points).

2.4. Histopathology

The joint tissues of the forepaws were harvested from the mice. The specimens were fixed in 4% paraformaldehyde and subsequently processed to prepare paraffin-embedded sections. The sections were stained with hematoxylin and eosin (H&E) for inflammation scoring and toluidine blue (TB) for cartilage degradation scoring. TB staining and evaluation methods were based on the method described by Maletzke et al. [22] with some modifications.

 doi:10.20944/preprints202409.1444.v

2.5. Immunohistochemistry

The immunohistochemistry analysis was performed according to the method described by Svendsen et al. [23] with some modifications. Briefly, the joint tissues of the forepaws of CAIA mice were fixed with 4% paraformaldehyde and subsequently processed to prepare paraffin-embedded sections. The fixed sections were blocked with 1.0% skim milk in PBS. Samples were incubated with rabbit anti-CD68 (staining for total macrophages), anti-CD80 (staining for M1-type macrophages) and anti-CD206 (staining for M2- type macrophages) primary antibodies, followed by Histofine Simple Stain Mouse MAX-PO (rabbit). The reaction was visualized using 3,3-diaminobenzidine tetrahydrochloride (DAB), and then the sections were counterstained with Harris hematoxylin. Slides were observed under an optical microscope (BZ-X800; KEYENCE). The immunostained samples were analyzed using ImageJ software (NIH Software).

2.6. Quantitative Real-Time Polymerase Chain Reaction (qRT-PCR) Analysis

qRT-PCR analysis was performed as described previously [24]. Briefly, total RNA was extracted from the joints of the rear paws using TRI reagent (Molecular Research Center Inc. Cincinnati, OH, USA). Reverse transcription was performed using oligo(dT) 15 primer (Promega, Tokyo, Japan) and Revertra Ace (Toyobo, Osaka, Japan). qRT-PCR was conducted using a Quantstudio3 system (Applied Biosystems, Waltham, MA, USA). The cDNA was amplified using Brilliant III Ultra-Fast SYBR Green QPCR Master Mix (Agilent Technologies, Hachioji, Tokyo, Japan). The following primer sets were utilized.

Gapdh, forward: AAATGGTGAAGGTCGGTGTG and reverse: TGAAGGGGTCGTTGATGG; *Tnfa*, forward: ACGCTGATTTGGTGACCAGG and reverse: GACCCGTAGGGCGATTACAG; *Il1b*, forward: ACCTAGCTGTCAACGTGTGG and reverse: TCAAAGCAATGTGCTGGTGC; *Cd80*, forward: CAAGTTTCCATGTCCAAGGC and reverse: GGCAAGGCAGCAATACCTTA; *Mmp13*, forward: GATGGCACTGCTGACATCAT and reverse: TTGGTCCAGGAGGAAAAGC; *Il6*, forward: CCCCAATTTCCAATGCTCTCC and reverse: CGCACTAGGTTTGCCGAGTA; *Col1a1*, forward: TGTTCAGCTTTGTGGACCTC and reverse: TCAAGCATACCTCGGGTTTC; *Col2a1*, forward: GGTCCCCCTGGCCTTAGT and reverse: CCTTGCATGACTCCCATCTG; *Sox9*, forward: AAGACTCTGGGCAAGCTCTG and reverse: GGGCTGGTACTTGTAATCGGG; *Acan*, forward: CAATTACCAGCTGCCCTTCA and reverse: CAGGGAGCTGATCTCGTAGC; *Sp7*, forward: GCCCCCTGGTGTTCTTCATT and reverse: CCCATTGGACTTCCCCCTTC; *Runx2*, forward: GTGGCCACTTACCACAGAGC and reverse: TGAGGCGATCAGAGAACAAA; *Acp5*, forward: GGTATGTGCTGGCTGGAAAC and reverse: ATTTTGAAGCGCAAACGGTA; *Ctsk*, forward: GTCGTGGAGGCGGCTATATG and reverse: AGAGTCAATGCCTCCGTTCTG. The mRNA levels of each transcript were determined relative to the expression levels of the housekeeping gene Gapdh.

2.7. Micro-Computed Tomography (μ-CT)

The method used for μ-CT analysis was based on the procedure described by Maleitzke et al. [25] with some modifications. The radiocarpal region with a slice thickness of 2.5 μm was analyzed using a μ-CT SkyScan 1272 scanner (Bruker, MA, USA). The analysis region was evaluated within a width of 0.5 mm immediately below the growth plate cartilage. The evaluated bone parameters included the percent bone volume (BV/TV), bone volume fraction (BS/TV), bone surface-to-volume ratio (BS/BV), trabecular number (Tb. N), trabecular thickness (Tb. Th), trabecular separation (Tb. Sp), trabecular bone pattern (Tb. Pf), structural model index (SMI), degree of anisotropy (DA), fractal dimension (FD), connectivity density (Conn. D), and bone mineral density (BMD). NRecon reconstruction software (SkyScan, Bruker) was used for section reconstruction, and 3D image reconstruction was performed using the CTVOX (Bruker) software.

2.8. Statistical Analysis

Quantitative data are presented as mean ± standard deviation (SD), except for the arthritis score, which is presented as the standard error of the mean (SEM). The Tukey-Kramer method was used to

 doi:10.20944/preprints202409.1444.v

identify differences between each experimental group when a significant difference (*$P < 0.05$ or **$P < 0.01$) was determined using analysis of variance (ANOVA).

3. Results

3.1. Rab44 Deficiency Attenuates Macroscopic Inflammation Induced by Collagen Antibody-Induced Arthritis (CAIA)

To test whether Rab44 is involved in the development of inflammation during arthritis, we induced CAIA in WT and Rab44-KO mice. Figure 1a shows the time course of the CAIA experiments. Upon the CAIA induction, the WT mice displayed severe arthritis in both the fore and hind paws, including the elbow and knee joints (Figure 1b). However, compared to the WT mice, Rab44-KO CAIA mice exhibited impaired arthritis phenotypes, such as edema and redness (Figure 1b). Quantification of arthritis scores revealed that Rab44-KO CAIA mice had an arthritis score approximately half that of WT CAIA mice (Figure 1c). These data indicate that Rab44 deficiency attenuates the macroscopic inflammation induced by CAIA.

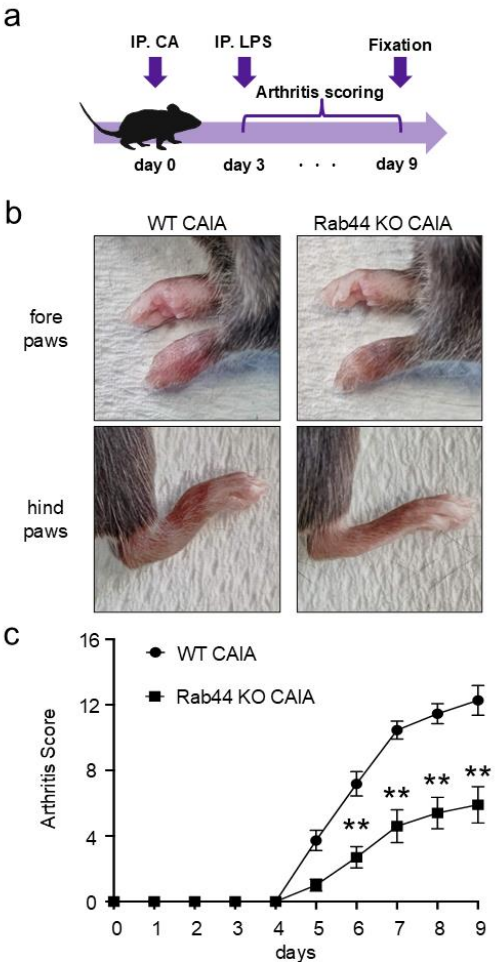

Figure 1. Development of collagen antibody-induced arthritis (CAIA) Wild type (WT) and Rab44-knockout (KO) mice were intraperitoneally injected with collagen II antibody cocktail (2 mg) on day 0; subsequently they were intraperitoneally injected with lipopolysaccharide (LPS) (50 μg) on day 3. The mice were monitored for arthritis development during 0-9 days by daily scoring. (a) Schematic diagram showing the time course for creating CAIA mice. (b) Photographs of the fore and hind paws of WT and Rab44- KO CAIA mouse on day 9. (c) Arthritis scores of the WT and Rab44- KO CAIA mice. Scoring was calculated with a maximum of 16 points, with four points assigned per paw (no swelling, 0 points; mild swelling and/or one swollen joint, 1 point; moderate swelling and/or two

 doi:10.20944/preprints202409.1444.v

swollen joints, 2 points; marked swelling and/or redness in all swollen joints, 3 points; severe swelling with redness in all swollen joints, 4 points). WT: n=11, Rab44 KO: n=10, ** p<0.01.

3.2. Rab44 KO CAIA Mice Exhibit Reduced Cell Filtration in the Radiocarpal Joints

Next, we performed a histopathological analysis of WT and Rab44-KO CAIA mice. Histopathological analysis of the radiocarpal joints using H&E staining showed significant infiltration with marked soft tissue edema and synovial lining cell hyperplasia in WT CAIA mice (Figure 2a). However, mild inflammatory infiltration with no soft tissue edema or synovial lining cell hyperplasia was observed in Rab44-KO CAIA mice (Figure 2a). Between WT and Rab44 KO control mice, there was no significant morphological difference (Figure 2a). Quantification of the inflammation scores between WT and Rab44-KO CAIA mice revealed significantly reduced scores in Rab44-KO CAIA mice (Figure 2b).

To assess the extent of cartilage degradation, histopathological analysis using toluidine blue staining was performed. WT CAIA mice showed thinning of the cartilage staining layer and decreased staining intensity, particularly in the metacarpophalangeal joint, indicating moderate cartilage degradation (Supplementary Figure 1a). In Rab44-KO CAIA mice, changes in staining intensity and size of stained cartilage layer were less pronounced than those in WT CAIA mice (Supplementary Figure 1a). However, in the quantitative evaluation using the cartilage degradation score, no significant difference was observed between WT and Rab44-KO CAIA mice (Supplementary Figure 1b).

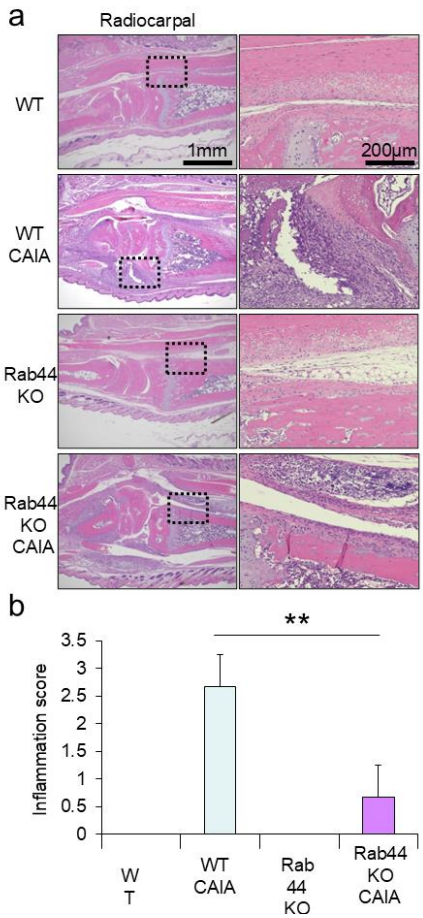

Figure 2. Histological analysis of radiocarpal joints of mice. (a) Hematoxylin and eosin (H&E) staining of radiocarpal joints of wild-type (WT) control, WT collagen antibody-induced arthritis (CAIA), Rab44-knockout (KO) control, and Rab44- KO CAIA mice. The dotted lines in the left panel are shown enlarged in the right panel. (b) Inflammation scores were counted with H&E staining histological data. Score 0, normal; Score1, mild cell infiltration with no soft tissue edema or synovial lining cell

 doi:10.20944/preprints202409.1444.v

hyperplasia; Score 2, moderate cell infiltration with surrounding soft tissue edema and some synovial lining cell hyperplasia; Score 3, severe cell infiltration with marked soft tissue edema and synovial lining cell hyperplasia (n=3, **p <0.01).

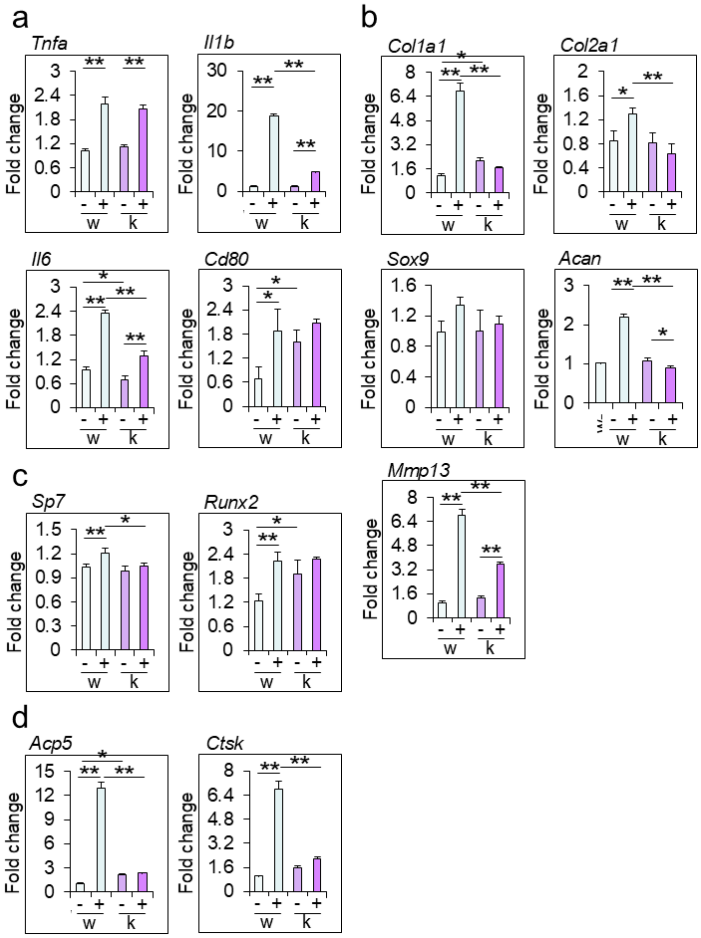

Figure 3. mRNA levels of arthritis marker genes in the ankle joints of mice mRNA was extracted from the ankle joints of wild-type (WT) control (w-), WT collagen antibody-induced arthritis (CAIA) (w+), Rab44-knockout (KO) control (k-), and Rab44- KO CAIA mice (k+). Subsequently, qRT-PCR was performed. (a) inflammatory markers, tumor necrosis factor-α (Tnfa), interleukin-1β (Il1b), interleukin-6 (Il6), and CD80 (Cd80). (b) cartilage turnover markers collagen type Ⅰα1 chain (Col1a1), collagen type Ⅱα1 chain (Col2a1), SRY-Box transcription factor 9 (Sox9), aggrecan (Acan) and matrix metalloprotease 13 (Mmp13). (c) Bone formation markers, Sp7 transcription factor (Sp7) and RUNX family transcription factor 2 (Runx2). (d) Bone resorption markers, tartrate-resistant acid phosphatase type 5 (Acp5) and cathepsin K (Ctsk). (*p<0.05, **p <0.01).

3.3. Rab44-KO CAIA Mice Show Decreased Expression Levels of Arthritis-Related Marker Genes

To investigate the effects of Rab44 on inflammation and turnover of cartilage and bone, we determined the mRNA levels of marker genes in the ankle joints of WT and Rab44-KO CAIA mice (Figure 3). The mRNA levels of inflammation genes, such as tumor necrosis factor-α (*Tnfa*), interleukin-1β (*Il1b*), interleukin-6 (*Il6*), and CD80 (*Cd80*) in WT and Rab44-KO CAIA joints were all significantly higher than those in the respective WT and Rab44-KO control joints (Figure 3a). Notably, the levels of *Il1b* and *Il6* in KO CAIA mice were significantly lower than those in WT CAIA mice (Figure 3a). However, mRNA levels of *Tnfa* between the WT and Rab44-KO CAIA mice were comparable (Figure 3a). Interestingly, in Rab44-KO control mice, the mRNA levels of *Il6* were lower but those of *Cd80* were higher than those in WT control mice (Figure 3a).

The mRNA levels of the cartilage turnover genes, including collagen type Ⅰα1 chain (*Col1a1*), collagen type Ⅱα1 chain (*Col2a1*), aggrecan (*Acan*) and matrix metalloprotease 13 (*Mmp13*) in WT

 doi:10.20944/preprints202409.1444.v

CAIA mice were significantly higher than those of WT control mice (Figure 3b). However, the levels of *Col1a1* and *Col2a1* in Rab44-KO CAIA mice were similar to those in Rab44-KO control mice, although the levels of Mmp13 in Rab44-KO CAIA mice were significantly higher than in Rab44-KO control mice (Figure 3b). Moreover, the mRNA levels of *Acan* in Rab44-KO CAIA mice were significantly lower than those in Rab44-KO control mice (Figure 3b). Importantly, the mRNA levels of *Col1a1*, *Col2a1*, *Acan* and *Mmp13* in Rab44-KO CAIA mice were significantly lower than those in WT CAIA mice (Figure 3b). However, the levels of SRY-Box transcription factor 9 (*Sox9*) in WT and KO mice were indistinguishable, with or without CAIA induction (Figure 3b).

The mRNA levels of bone formation genes, such as Sp7 transcription factor (Sp7) and RUNX family transcription factor 2 (*Runx2*), in WT CAIA mice were significantly higher than those in (Figure 3c). However, both *Sp7* and Runx2 levels were similar between Rab44-KO control and CAIA mice (Figure 3c). Similarly, the levels of bone resorption genes, including tartrate-resistant acid phosphatase type 5 (*Acp5*) and cathepsin K (*Ctsk*) in WT CAIA mice were markedly increased compared to those in the WT control mice (Figure 3d). However, *Acp5* and *Ctsk* levels in Rab44-KO mice were indistinguishable between before and after CAIA induction (Figure 3d).

3.4. Rab44-KO CAIA Mice Exhibit Predominant Filtration of M2-Type Macrophages at the Inflammatory Sites

To further investigate the mechanisms of reduced inflammation in Rab44-KO CAIA mice, we examined macrophage subtypes by immunohistochemical analysis (Figure 4). Macrophages are polarized into two subtypes: classically activated macrophages (M1) and alternatively activated macrophages (M2), which have anti-inflammatory activities [26,27]. We selected three different markers: CD68 is a marker for recognizing both M1 and M2 macrophages [28]. CD80 is an M1-type marker [29], and CD206 is an M2-type marker [30]. Immunohistochemical analysis showed that the number of CD68-positive macrophages in Rab44CAIA mice was apparently lower than that in WT CAIA mice (Figure 4a). The quantitative analysis of CD68-positive macrophages also was consistent with these data (Figure 4b, left panel.). Immunohistochemical and quantitative analyses revealed that the number of CD80-positive macrophages (M1) in Rab44-KO CAIA mice was significantly lower than that in WT CAIA mice (Figure 4a and b, middle panel). Conversely, the number of CD206-positive macrophages (M2) in Rab44-KO CAIA mice was significantly higher than that in WT CAIA mice (Figure 4a, 4b, left panel). These results indicate that Rab44-KO CAIA mice exhibit predominant filtration of M2-type macrophages at the inflammatory sites, although they show reduced filtration of total macrophages.

3.5. Rab44 KO CAIA Mice Display Impaired Bone Loss Compared with WT CAIA Mice

Finally, we analyzed the morphological changes in the trabecular bone of the radiocarpal joints of WT and Rab44-KO CAIA mice using micro-computed tomography (μ-CT) (Figure 5a). Upon reconstructing 3D images and color-coding them based on CT values, Rab44-KO CAIA mice showed bone structures with higher CT values than WT CAIA mice (Figure 5b). Radiocarpal trabecular bone volume (BV/TV) fractions were significantly decreased in both types of CAIA mice compared with both groups of control mice (Figure 5c). Moreover, a comparison of various parameters between WT control and WT CAIA mice showed a significant decrease in the bone volume fraction (BS/TV), trabecular number (Tb. N), and fractal dimension (FD), as well as a significant increase in trabecular separation (Tb. Sp), trabecular bone pattern (Tb. Pf), connectivity density (Conn. D), and structure model index (SMI) after CAIA induction (Figure 5c and Supplementary Figure 2). However, all parameters except for bone surface to volume (BS/BV), Tb. Pf and SMI, were indistinguishable between the Rab44-KO CAIA and KO control mice. (Figure 5c and Supplementary Figure 2). In addition, the five indices, including BS/TV, Tb. N, Tb. Sp, FD, and Conn D indicated reduced bone loss in Rab44-KO CAIA mice was observed compared with WT CAIA mice (Figure 5c). These results indicate that Rab44-KO CAIA mice display impaired bone loss compared to WT CAIA mice.

 doi:10.20944/preprints202409.1444.v

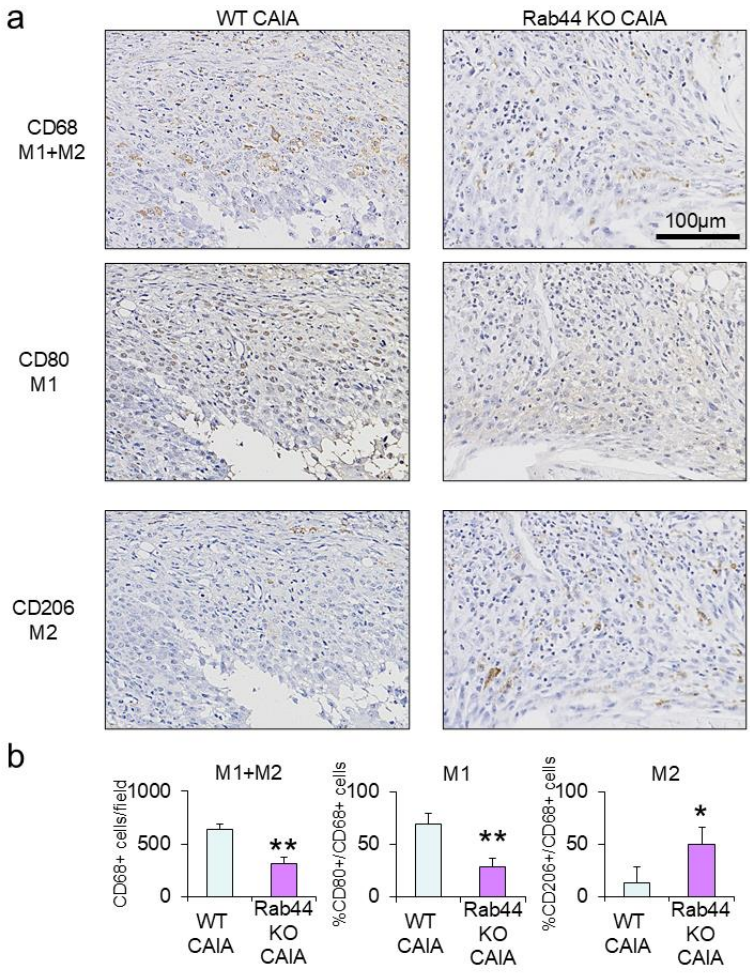

Figure 4. Immunohistochemical analysis of M1 and/orM2 type macrophages in the joint of collagen antibody-induced arthritis (CAIA) mice (a) The fixed sections of wild-type (WT) and Rab44-knockout (KO) CAIA mice were blocked with 1.0% skim milk in PBS. The samples were incubated with rabbit anti-CD68 IgG (total macrophage marker), CD80 IgG (M1-type macrophage marker) and CD206 IgG (M2- type macrophage marker) as the primary antibodies, followed by an HRP/DAB detection method. Samples were observed under an optical microscope. Bars: 100 μm. (b) Quantitative analysis of the serial sections with the number of CD68-positive cells visualized in a certain field (left panel), the percentage of the number of CD80-positive cells in the number of CD68-positive cells (middle panel), and the percentage of the number of CD206-positive cells in the number of CD68-positive cells (right panel). Data are represented as the mean ± S.E. of results from three independent experiments. Asterisks indicate statistical significance compared to the control; (n=4, *$p<0.05$, **$p<0.01$).

 doi:10.20944/preprints202409.1444.v

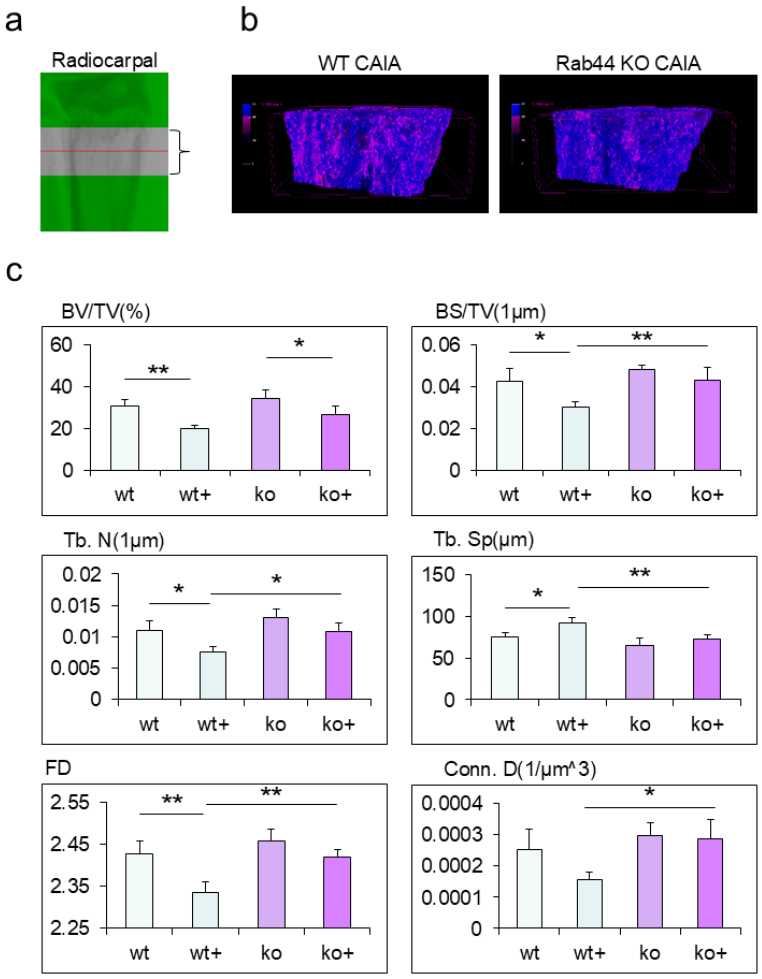

Figure 5. Micro-computed tomography (μ-CT) analysis of the trabecular bone of the radiocarpal joints of mice The trabecular bones of wild-type (WT) control (w-), WT collagen antibody-induced arthritis (CAIA) (w+), Rab44-knockout (KO) control (k-), and Rab44- KO CAIA mice (k+) were analyzed using μ-CT. (a) The analyzed area of the trabecular bone by μ-CT. Distal radius 0.5 mm length. (b) Representative 3D μ-CT images of trabecular bone at the distal radius, colour-coded according to CT value. Areas where the CT values were lower than others are shown in reddish-purple. (c) Results showing percent bone volume (BV/TV), bone volume fraction (BS/TV), trabecular number (Tb. N), trabecular separation (Tb. Sp) fractal dimension (FD), and connectivity density (Conn. D) of the trabecular bones at distal end of radius in wild-type (WT) control (w-), WT collagen antibody-induced arthritis (CAIA) (w+), Rab44-knockout (KO) control (k-), and Rab44- KO CAIA mice (k+), (n=4, *p<0.05, **p <0.01).

4. Discussion

In this study, we demonstrated that Rab44 deficiency attenuated CAIA-induced macroscopic inflammation. Histopathological analyses revealed that Rab44 KO CAIA mice exhibited reduced cell filtration in the radiocarpal joints. Real-time PCR analyses indicated that Rab44-KO CAIA mice exhibited decreased expression levels of arthritis-related marker genes. Immunohistochemical analysis showed that Rab44-KO CAIA mice exhibited predominant filtration of M2-type macrophages at inflammatory sites. Micro-CT analyses revealed that Rab44 KO CAIA mice displayed impaired bone loss compared to WT CAIA mice. Thus, Rab44 deficiency likely reduces the progression of inflammation in CAIA in mice.

Consistent with the findings of this study, previous *in vivo* studies have indicated that Rab44-KO mice display impaired allergic responses, such as anaphylactic responses and nickel-induced

 doi:10.20944/preprints202409.1444.v

hypersensitivity [18,19]. *In vitro* studies on bone marrow mast cells derived from Rab44-KO mice showed reduced secretion of histamine and β-hexosaminidase compared to those from WT mice. Moreover, Rab44-KO mice exhibited slightly impaired production of TNF-α and interleukin-10 after LPS stimulation [19]. Genetic studies have suggested that human *Rab44* is involved in immune diseases. A study using transcriptome data reported that immune patients with atopy and atopic asthma have differential expression levels of the *Rab44* gene compared to normal individuals [31]. In addition to allergies, Rab44 is likely to be involved in autoimmune diseases. A study using whole-genome sequencing study reported that a missense mutation in the Rab44 gene was found in T cells from patients with the autoimmune CD4-lymphoproliferative disease [32]. Considering that Rab44 KO mice exhibit lower levels of CAIA induced inflammation, it is likely that Rab44 deficiency reduces wide-range immune responses, such as allergies and autoimmune diseases.

The present *in vivo* study demonstrated that Rab44-KO CAIA mice showed decreased mRNA levels of osteoclasts, such as Acp5 and Ctsk. In contrast, our previous *in vitro* study indicated that Rab44 knockdown promoted osteoclast differentiation and enhanced bone resorption [14]. The discrepancy in these findings between previous *in vitro* and present in vivo studies would explain why the upstream effects, including decreased production of cytokines and chemical mediators by Rab44-KO mice, affected the downstream effects such as decreased levels of the osteoclast markers Acp5 and Ctsk and decreased morphological bone destruction. Consistent with this, previous studies have demonstrated that Rab44-KO mice exhibited reduced inflammatory responses. In fact, Rab44-KO mice exhibited slightly impaired production of TNF-α and interleukin-10 after LPS stimulation [19], and mast cells from Rab44-KO mice showed reduced secretion of histamine and β-hexosaminidase compared to WT mice [18]. Therefore, even if Rab44 deficiency increased osteoclast differentiation and activity in vitro, when the upstream inflammatory response is attenuated in vivo, osteoclast differentiation and bone resorption ability would also be impaired.

Predominant filtration of M2-type macrophages at inflammatory sites was observed in Rab44-KO CAIA mice. Our *in vitro* studies indicated that Rab44 is upregulated during the early phase of differentiation of M1- and M2-type macrophages [19]. Treatment of human macrophage THP1 cells with LPS and interferon-γ (M1 induction) or IL-4 and IL-13 (M2 induction) increases the expression levels of Rab44 in the early phase [19]. However, the detailed mechanisms underlying the involvement of Rab44 in the polarization of M1 and M2 macrophages remain unclear. Therefore, Rab44 may be involved in immune cell differentiation. This hypothesis is based on several findings. First, Rab44 expression levels are decreased during the differentiation of mature immune cells. such as macrophages, neutrophils, and dendritic cells, whereas Rab44 is highly expressed in undifferentiated hematopoietic cells of the bone marrow [16]. Alternatively, after treatment with LPS, Rab44 is partially translocated into early endosomes and the plasma membrane, whereas Rab44 is mainly localized in lysosomes of macrophages [16]. Thus, it is important to determine the mechanisms underlying Rab44 involvement in the polarization of M1 and M2 macrophages in future studies.

5. Conclusions

In conclusion, Rab44 KO CAIA mice exhibited reduced inflammation and total macrophage filtration but increased M2-type macrophage filtration. Consistent with these findings, Rab44-KO CAIA mice showed decreased expression levels of arthritis-related marker genes, and impaired bone loss compared to WT CAIA mice. Thus, it is likely that Rab44 deficiency reduces the progression of inflammation in CAIA in mice.

Supplementary Materials: The following supporting information can be downloaded at: www.mdpi.com/xxx/s1, Figure S1 and Figure S2.

Author Contributions: Conceptualization, Y.Y. and T.T.; breeding and management of mice, Y.Y., T.K., M.N., S.O.; quantitative RT-PCR, Y.Y. and S.O.; histological analyses, Y.Y. and T.K. and M.N.; formal analysis, Y.Y., E.S. and T.T.; Y.Y. and T.T. writing—review and editing, funding acquisition, Y.Y., T.K., E.S. and T.T.; project administration, T.T. All authors have read and agreed to the published version of the manuscript.

Funding: This study was supported financially by the research grant of Astellas Foundation for Research on Metabolic Disorders, and partially by the JSPS KAKENHI grant numbers, 20H03860, 20K18459 22K17004 and 24K12899.

Statement of ethics: This study protocol was reviewed and approved by the Animal Experiment Committee of the Graduate School of Biomedical Sciences, Nagasaki University (permit number: 2107211733).

Data Availability Statement: The data used to support the findings of this study are available from the corresponding author upon request.

Conflicts of Interest: The authors declare no competing interests.

References

1. Scherer, H.U.; Häupl, T.; Burmester, G.R. The etiology of rheumatoid arthritis. *J Autoimmun* **2020**, 110, 102400.
2. Andreev, D.; Kachler, K.; Schett, G.; Bozec, A. Rheumatoid arthritis and osteoimmunology: The adverse impact of a deregulated immune system on bone metabolism. *Bone* **2022**, 162, 116468.
3. Komatsu, N.; Takayanagi, H. Mechanisms of joint destruction in rheumatoid arthritis - immune cell-fibroblast-bone interactions. *Nat Rev Rheumatol* **2022**, 18, 415-429.
4. Yap, H.Y.; Tee, S.Z.; Wong, M.M.; Chow, S.K.; Peh, S.C.; Teow, S.Y. Pathogenic Role of Immune Cells in Rheumatoid Arthritis: Implications in Clinical Treatment and Biomarker Development. *Cells* **2018**, *7*, 161.
5. Yang, M.; Zhu, L. Osteoimmunology: The Crosstalk between T Cells, B Cells, and Osteoclasts in Rheumatoid Arthritis. *Int J Mol Sci* **2024**, *25*, 2688.
6. Hashida, R.; Shimozuru, Y.; Chang, J.; Agosto-Marlin, I.; Waritani, T.; Terato, K. New Studies of Pathogenesis of Rheumatoid Arthritis with Collagen-Induced and Collagen Antibody-Induced Arthritis Models: New Insight Involving Bacteria Flora. *Autoimmune Dis* **2021**, 2021, 7385106.
7. Maleitzke, T.; Weber, J.; Hildebrandt, A.; Dietrich, T.; Zhou, S.; Tsitsilonis, S.; Keller, J. Standardized protocol and outcome measurements for the collagen antibody-induced arthritis mouse model. *STAR Protoc* **2022**, 3, 101718.
8. Kong, J.S.; Jeong, G.H.; Yoo, S.A. The use of animal models in rheumatoid arthritis research. *J Yeungnam Med Sci* **2023**, *40*, 23-29.
9. Hutagalung, A.H.; Novick, P.J. Role of Rab GTPases in membrane traffic and cell physiology. *Physiol Rev* **2011**, *91*, 119-149.
10. Zhen, Y.; Stenmark, H. Cellular functions of Rab GTPases at a glance. *J Cell Sci* **2015**, *128*, 3171-3176.
11. Homma, Y.; Hiragi, S.; Fukuda, M. Rab family of small GTPases: an updated view on their regulation and functions. *Febs j* **2021**, *288*, 36-55.
12. Tsukuba, T.; Yamaguchi, Y.; Kadowaki, T. Large Rab GTPases: Novel Membrane Trafficking Regulators with a Calcium Sensor and Functional Domains. *Int J Mol Sci* **2021**, *22*, 7691.
13. Maruta, Y.; Fukuda, M. Large Rab GTPase Rab44 regulates microtubule-dependent retrograde melanosome transport in melanocytes. *J Biol Chem* **2022**, *298*, 102508.
14. Yamaguchi, Y.; Sakai, E.; Okamoto, K.; Kajiya, H.; Okabe, K.; Naito, M.; Kadowaki, T.; Tsukuba, T. Rab44, a novel large Rab GTPase, negatively regulates osteoclast differentiation by modulating intracellular calcium levels followed by NFATc1 activation. *Cell Mol Life Sci* **2018**, *75*, 33-48.
15. Ogawa, K.; Kadowaki, T.; Tokuhisa, M.; Yamaguchi, Y.; Umeda, M.; Tsukuba, T. Role of the EF-hand and coiled-coil domains of human Rab44 in localisation and organelle formation. *Sci Rep* **2020**, *10*, 19149.
16. Tokuhisa, M.; Kadowaki, T.; Ogawa, K.; Yamaguchi, Y.; Kido, M.A.; Gao, W.; Umeda, M.; Tsukuba, T. Expression and localisation of Rab44 in immune-related cells change during cell differentiation and stimulation. *Sci Rep* **2020,** 10, 10728.
17. Kadowaki, T.; Yamaguchi, Y.; Ogawa, K.; Tokuhisa, M.; Okamoto, K.; Tsukuba, T. Rab44 isoforms similarly promote lysosomal exocytosis, but exhibit differential localization in mast cells. *FEBS Open Bio* **2021**, 11, 1165-1185.
18. Kadowaki, T.; Yamaguchi, Y.; Kido, M.A.; Abe, T.; Ogawa, K.; Tokuhisa, M.; Gao, W.; Okamoto, K.; Kiyonari, H.; Tsukuba, T. The large GTPase Rab44 regulates granule exocytosis in mast cells and IgE-mediated anaphylaxis. *Cell Mol Immunol* **2020**, 17, 1287-1289.
19. Noguromi, M.; Yamaguchi, Y.; Sato, K.; Oyakawa, S.; Okamoto, K.; Murata, H.; Tsukuba, T.; Kadowaki, T. Rab44 Deficiency Induces Impaired Immune Responses to Nickel Allergy. *Int J Mol Sci* **2023**, *24*, 994.
20. Longé, C.; Bratti, M.; Kurowska, M.; Vibhushan, S.; David, P.; Desmeure, V.; Huang, J.D.; Fischer, A.; de Saint Basile, G.; Sepulveda, F.E.; et al. Rab44 regulates murine mast cell-driven anaphylaxis through kinesin-1-dependent secretory granule translocation. *J Allergy Clin Immunol* **2022**, *150*, 676-689.
21. Oyakawa, S.; Yamaguchi, Y.; Kadowaki, T.; Sakai, E.; Noguromi, M.; Tanimoto, A.; Ono, Y.; Murata, H.; Tsukuba, T. Rab44 deficiency accelerates recovery from muscle damage by regulating mTORC1 signaling and transport of fusogenic regulators. *J Cell Physiol* **2023**, *238*, 2253-2266.

22. Maleitzke, T.; Hildebrandt, A.; Dietrich, T.; Appelt, J.; Jahn, D.; Otto, E.; Zocholl, D.; Baranowsky, A.; Duda, G.N.; Tsitsilonis, S.; et al. The calcitonin receptor protects against bone loss and excessive inflammation in collagen antibody-induced arthritis. *iScience* **2022**, *25*, 103689.
23. Svendsen, P.; Etzerodt, A.; Deleuran, B.W.; Moestrup, S.K. Mouse CD163 deficiency strongly enhances experimental collagen-induced arthritis. *Sci Rep* **2020**, *10*, 12447
24. Tanimoto, A.; Yamaguchi, Y.; Kadowaki, T.; Sakai, E.; Oyakawa, S.; Ono, Y.; Yoshida, N.; Tsukuba, T. Rab44 negatively regulates myoblast differentiation by controlling fusogenic protein transport and mTORC1 signaling. *J Cell Biochem* **2023**, *124*, 1486-1502.
25. Maleitzke, T.; Hildebrandt, A.; Weber, J.; Dietrich, T.; Appelt, J.; Jahn, D.; Zocholl, D.; Baranowsky, A.; Duda, G.N.; Tsitsilonis, S.; et al. Proinflammatory and bone protective role of calcitonin gene-related peptide alpha in collagen antibody-induced arthritis. *Rheumatology (Oxford)* **2021**, *60*, 1996-2009.
26. Martinez, F.O.; Gordon, S. The M1 and M2 paradigm of macrophage activation: time for reassessment. *F1000prime reports* **2014**, *6*, 13.
27. Yunna, C.; Mengru, H.; Lei, W.; Weidong, C. Macrophage M1/M2 polarization. Eur J Pharmacol **2020**, *877*, 173090.
28. Zhu, L.J.; Dai, L.; Zheng, D.H.; Mo, Y.Q.; Ou-Yang, X.; Wei, X.N.; Shen, J.; Zhang, B.Y. Upregulation of tumor necrosis factor receptor-associated factor 6 correlated with synovitis severity in rheumatoid arthritis. *Arthritis Res Ther* **2012**, *14*, R133.
29. Aota, K.; Yamanoi, T.; Kani, K.; Nakashiro, K.I.; Ishimaru, N.; Azuma, M. Inverse correlation between the number of CXCR3(+) macrophages and the severity of inflammatory lesions in Sjögren's syndrome salivary glands: A pilot study. *J Oral Pathol Med* **2018**, *47*, 710-718.
30. Bailey, K.N.; Furman, B.D.; Zeitlin, J.; Kimmerling, K.A.; Wu, C.L.; Guilak, F.; Olson, S.A. Intra-articular depletion of macrophages increases acute synovitis and alters macrophage polarity in the injured mouse knee. *Osteoarthritis Cartilage* **2020**, *28*, 626-638.
31. Jiang, Y.; Gruzieva, O.; Wang, T.; Forno, E.; Boutaoui, N.; Sun, T.; Merid, S.K.; Acosta-Pérez, E.; Kull, I.; Canino, G.; et al. Transcriptomics of atopy and atopic asthma in white blood cells from children and adolescents. *Eur Respir J* **2019**, *53*,1900102.
32. Comrie, W.A.; Faruqi, A.J.; Price, S.; Zhang, Y.; Rao, V.K.; Su, H.C.; Lenardo, M.J. RELA haploinsufficiency in CD4 lymphoproliferative disease with autoimmune cytopenias. *J Allergy Clin Immunol* **2018**, *141*, 1507-1510.